ACADEMIC PRESS

Available online at www.sciencedirect.com

SCIENCE DIRECT®

Journal of Catalysis 218 (2003) 220–226

JOURNAL OF CATALYSIS

www.elsevier.com/locate/jcat

Catalytic reduction of N_2O by C_2H_4 over Fe-ZSM-5: formation and nature of carbonaceous deposits and influence of the addition of O_2

T. Chaki,[a] M. Arai,[a] T. Ebina,[b] and M. Shimokawabe [a,*]

[a] Division of Materials Science and Engineering, Graduate School of Engineering, Hokkaido University, Sapporo 060-8628, Japan
[b] National Institute of Advanced Industrial Science and Technology, Sendai 983-8551, Japan

Received 9 December 2002; revised 12 February 2003; accepted 10 March 2003

Abstract

The catalytic reduction of dinitrogen monoxide (N_2O) by ethylene (C_2H_4) in the absence and presence of O_2 is studied over Fe-ZSM-5 catalysts. Two types of carbonaceous deposits ($C\alpha$, $C\beta$) are formed on Fe-ZSM-5 during the reduction of N_2O by C_2H_4 in the absence of O_2. The catalytic activity of Fe-ZSM-5 decreases with an increase in the amount of $C\alpha$, while the catalytic activity is not affected by the presence of $C\beta$. The formation of these carbonaceous deposits is suppressed by the presence of O_2 in the feed gas, and the catalytic reduction of N_2O by C_2H_4 is promoted by O_2, since deactivation of Fe sites is prevented in the presence of O_2.

Keywords: Fe-ZSM-5; N_2O reduction; Ethylene; Carbonaceous deposit; Temperature-programmed oxidation

1. Introduction

Dinitrogen monoxide (N_2O) is well known to be a greenhouse gas component and to contribute to the catalytic destruction of ozone in the stratosphere. The removal of N_2O by suitable catalytic methods has been a very important subject in order to protect the global environment. Recently, several research groups have reported high catalytic performance of various metal ion-exchanged zeolites and metal-containing catalysts for decomposition [1–6] and reduction of N_2O with hydrocarbons [7–15], activated carbon [16–18], CO [19,20], and NH_3 [21,22]. Segawa and co-workers [9–11] studied the selective reduction of N_2O using C_3H_6 as reductant and reported a high reaction rate over Fe-MFI even in the presence of oxygen and water vapor. In our previous paper [12], the catalytic reduction of N_2O using CH_4 and C_3H_6 as reductants in the presence and absence of oxygen was studied with 12 metal ion-exchanged ZSM-5 catalysts. Pronounced activities were observed with Fe-ZSM-5, Pd-ZSM-5, and Pt-ZSM-5 catalysts. No significant deactivation was detected with Fe-ZSM-5 in the presence of O_2, whereas the pronounced activities of Pt- and Pd-ZSM-5 were decreased drastically by the presence of 5% O_2. We assumed that the differences in the catalytic activity between Fe-ZSM-5 and Pd-ZSM-5 on N_2O reduction with CH_4 in the presence of O_2 may be explained in terms of the reactivity of O_2 with CH_4. Kameoka et al. [13–15] reported that the selective catalytic reduction of N_2O with CH_4 and C_3H_6 in the presence of excess O_2 occurs effectively over ion-exchanged Fe-BEA and Fe-MFI. The authors found the formation of carbon-containing surface species during the N_2O reduction with C_3H_6 and suggested that these species may be the active species for the N_2O reduction. Zhu and co-workers [16] reported that the activity of Cu- or Co-loaded activated carbon in N_2O conversion was better than that of Cu/ZSM-5 or Co/ZSM-5, respectively. They [17,18] also investigated the role of O_2 in the NO– and N_2O–carbon reactions and reported that the presence of O_2 greatly enhanced NO–carbon reactions while it depressed N_2O–carbon reactions on carbon surfaces. The catalytic combustion of hydrocarbons and the models of soot formation and oxidation have been extensively studied and were reviewed [23–25]. However, little fundamental study exists pertaining to the reduction of N_2O by carbon species including reaction intermediates in the presence of O_2 over metal zeolites.

In the present study, the reduction of N_2O with C_2H_4 under various reaction conditions has been studied over Fe-ZSM-5. The nature and structure of carbonaceous deposits

---

[*] Corresponding author.
E-mail address: shimo@proc-ms.eng.hokudai.ac.jp (M. Shimokawabe).

0021-9517/03/$ – see front matter © 2003 Elsevier Inc. All rights reserved.
doi:10.1016/S0021-9517(03)00121-0

formed on the catalyst have been investigated in the presence and absence of O_2 and the mechanism for the rate promotion with O_2 is discussed in terms of the activity of carbonaceous deposits formed on the catalyst.

2. Experimental

2.1. Catalyst preparation

Fe-ZSM-5 catalysts were prepared by a conventional ion-exchange method using Na-ZSM-5 ($SiO_2/Al_2O_3 = 23.8$) supplied from Tohso Co.Ltd. Na-ZSM-5 (4 g) was added to 100 cm^3 of $FeSO_4 \cdot 7H_2O$ aqueous solution and then stirred for 12 h at 343 K. After filtration, the metal-supported zeolites were washed with distilled water, dried at 383 K for 24 h, and calcined in air for 3 h at 773 K. $FeSO_4 \cdot 7H_2O$ aqueous solutions in concentration of 2.45×10^{-2}, 1.29×10^{-2}, and 7.17×10^{-3} M were used for preparing Fe-ZSM-5 with 3.4, 1.8, and 1.0 wt% Fe, respectively. A 3.4 wt% Fe corresponds to approximately 100% ion-exchange level. Unless otherwise stated, all the experiments were carried out using Fe-ZSM-5 (3.4 wt% Fe).

2.2. N_2O reduction

The reactant gases used were N_2O (2000, 4000, 6000, and 12,000 ppm) and C_2H_4 (2000, 4000, and 6000 ppm) diluted by He. For elucidation of the effect of O_2 on the reduction of N_2O, O_2 (1000, 2500, 5000, 10,000, and 15,000 ppm) was introduced in the feed gas. Prior to the runs, the catalysts were treated in the reactor at 773 K for 2 h and cooled to the reaction temperature in a stream of He. The reaction was carried out in a conventional flow reactor at a W/F of 0.06 $g\,s\,cm^{-3}$ and at 598 K. The reactor was made of 9-mm-diameter Pyrex glass tubing in which a catalyst sample of 0.05 g was mounted on loosely packed quartz wool. The concentrations of N_2O, N_2, O_2, CO, CO_2, and hydrocarbons in the outflow gas were determined using gas chromatographs (Hitachi 663-50 and 063) with Porapak Q and molecular sieve 5 Å columns. The concentration of NO_2 was monitored using a UV–Vis spectrophotometer (Hitachi Model 100-10). Because of the low concentrations of N_2O and hydrocarbons in the outflow, the total flow rate was practically constant throughout the catalyst bed.

2.3. Catalyst characterization

TPO (temperature-programmed oxidation) experiments were carried out in the same reactor as used above. After the reactions were carried out under various conditions, the reactor was cooled to room temperature, the stream of reactants was switched to He, and it was passed for 60 min. Programmed heating was then started from room temperature to 773 K at a rate of 5 $K\,min^{-1}$ in the stream of 5000 ppm O_2. The amounts of gases (CO, CO_2) evolved were estimated from the peak areas of TPO curves.

DRIFTS (diffuse reflectance infrared Fourier transform spectroscopy) spectra were recorded by means of a Fourier transform-infrared spectrophotometer (Nihon Bunko FT-IR5M) with a diffuse reflectance attachment (Nihon Bunko DG-500/H). The powdered catalyst was placed on a sample cell in the diffuse reflectance attachment. N_2O (8000 ppm) and C_2H_4 (8000 ppm) diluted with He were fed over the catalyst at 598 K for given periods of time. The IR measurement was then carried out at the same temperature as used for adsorption.

XPS (X-ray photoelectron spectroscopy) analysis was performed in a ULVAC PHI ESCA 5600 instrument. Mg-K_α radiation (14.0 kV, 400 W) was used to excite photoelectrons, which were detected with analyzer operated at 1253.6 eV constant pass energy. Correction of the energy shift, due to steady-state charging, was accomplished by taking the C 1s line from adsorbed carbons at 284.5 eV as an internal standard.

^{57}Fe Mössbauer spectra of catalysts were recorded at room temperature by an Austin S-600 instrument using ^{57}Co in a Rh matrix as a source. XRD (X-ray powder diffraction) patterns were taken using a Rigaku Rint 1000 instrument (Co-K_α radiation: 30 kV, 15 mA).

3. Results and discussion

3.1. Influence of the addition of O_2 on N_2O reduction

Fig. 1 shows typical results for the reduction of N_2O (2000 ppm) by C_2H_4 (2000 ppm) in the absence and presence of O_2 (5000 ppm) at 598 K. Under these conditions, three gases such as N_2, CO_2, and CO were observed to form as main products. In the absence of O_2, the partial pressures of these products decrease rapidly with time on stream at the initial stage of reaction and then they change gradually to steady-state values. When O_2 is added, however, the partial pressures of the products change little with time except for an initial short period and the product distribution is different from that observed in the absence of O_2. The steady-state conversion of N_2O to N_2 in the presence of O_2 is larger by a factor of 2 than that in the absence of O_2.

3.2. Formation and nature of carbonaceous deposits

Temperature-programmed oxidation was used to characterize chemical species formed on the surface of catalyst after N_2O reduction. Fig. 2 shows TPO curves of chemical species formed on Fe-ZSM-5 (3.4 wt% Fe) during the reduction of N_2O (2000 ppm) by C_2H_4 (2000 ppm) at 598 K in the absence of O_2. CO and CO_2 were observed to evolve, along with a trace amount of H_2O. The evolution peak of CO is seen at approximately 570 K and CO_2 peaks are seen at approximately 570 and around 670 K. The peaks centered

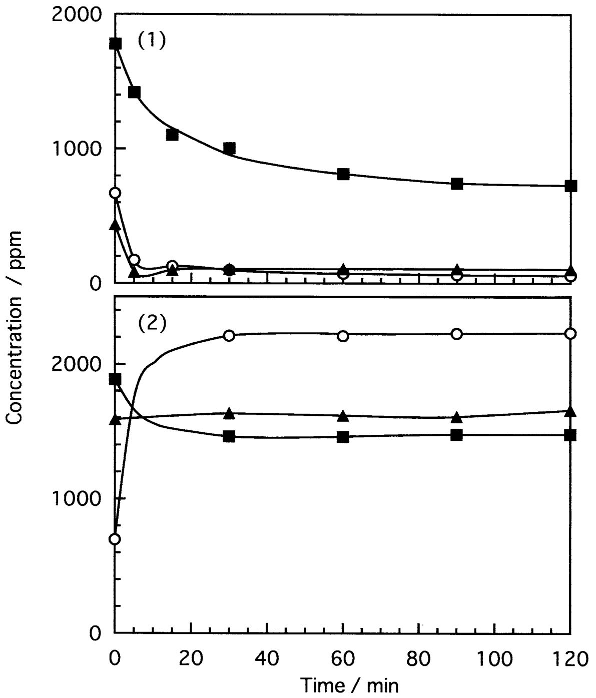

Fig. 1. The catalytic reduction of N_2O (2000 ppm) by C_2H_4 (2000 ppm) in the absence (1) and in the presence (2) of O_2 (5000 ppm) over Fe-ZSM-5 (3.4 wt% Fe) measured at 598 K (■, N_2; ▲, CO_2; ○, CO).

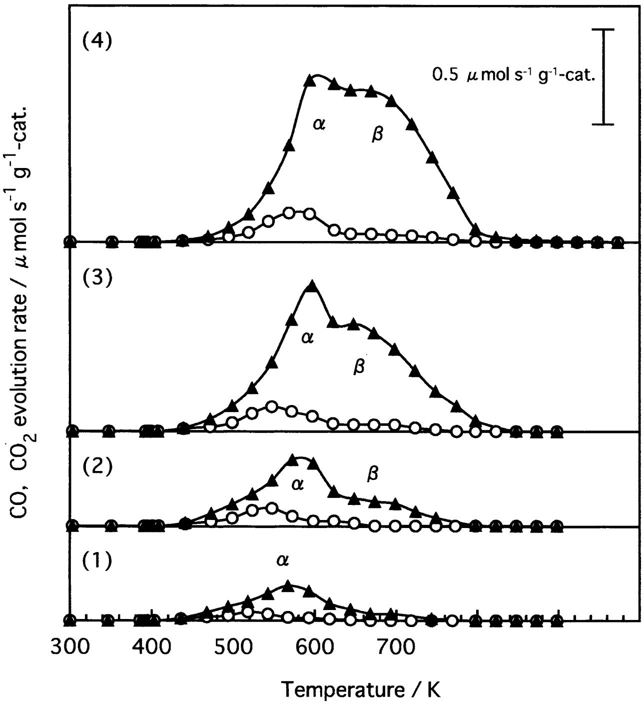

Fig. 2. TPO curves of the carbonaceous deposit accumulated on Fe-ZSM-5 (3.4 wt% Fe) during the N_2O reduction by C_2H_4 at 598 K for (1) 5 min, (2) 15 min, (3) 60 min, and (4) 120 min (○, CO; ▲, CO_2).

at temperatures of 570 and 670 K are henceforth referred to as α-peak and β-peak, respectively. CO_2 and CO evolved during the TPO run may be regarded as oxidation products of carbonaceous deposits accumulated on the surface of catalyst, since the amount of carbon of C_2H_4 consumed during the reduction is larger than that of the products (CO_2 and CO) and unreacted C_2H_4. Therefore, the carbonaceous deposits evolved as CO_2 and/or CO at α-peak and β-peak regions are named Cα and Cβ, respectively. On the basis of the results shown in Fig. 2, it is found that only Cα is formed over the catalyst during the N_2O reduction at 598 K for a short time (5 min). The amount of Cα increases with an increase in contact time and then approaches a constant level up to 60 min. On the other hand, a β-CO_2 peak is observed after 15 min and the amount of Cβ increases with an increase in contact time.

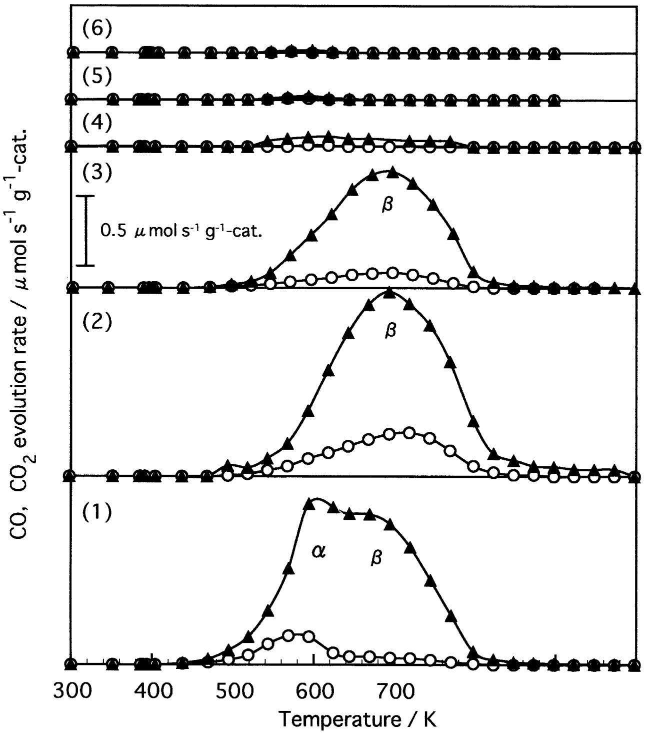

Fig. 3. TPO curves of the carbonaceous deposit accumulated on Fe-ZSM-5 (3.4 wt% Fe) during the N_2O reduction by C_2H_4 at 598 K for 2 h in the presence of (1) 0 ppm, (2) 1000 ppm, (3) 2500 ppm, (4) 5000 ppm, (5) 10000 ppm, and (6) 15000 ppm of O_2 (○, CO; ▲, CO_2).

The influence of the addition of O_2 into the feed gas was also investigated by means of TPO runs. Fig. 3 shows TPO curves of the carbonaceous deposits accumulated on Fe-ZSM-5 (3.4 wt% Fe) during the reduction of N_2O (2000 ppm) by C_2H_4 (2000 ppm) at 598 K for 2 h in the absence and presence of O_2. Fig. 3 (1) shows the same TPO curves as shown in Fig. 2 (4). It is seen that α-peaks of CO and CO_2 disappear in the presence of O_2 (1000 ppm) while β-CO and β-CO_2 peaks exist and the amount of Cβ decreases with an increase in the partial pressure of O_2 used. It is seen that a trace amount of Cβ is accumulated in the presence of 5000 ppm O_2 while the β-peak disappears in the presence of O_2 above 10,000 ppm.

Fig. 4 shows TPO curves for the carbonaceous deposits accumulated on Fe-ZSM-5 (3.4 wt% Fe) during the reduction of N_2O (2000 ppm) by C_2H_4 (2000 ppm) at 598 K in

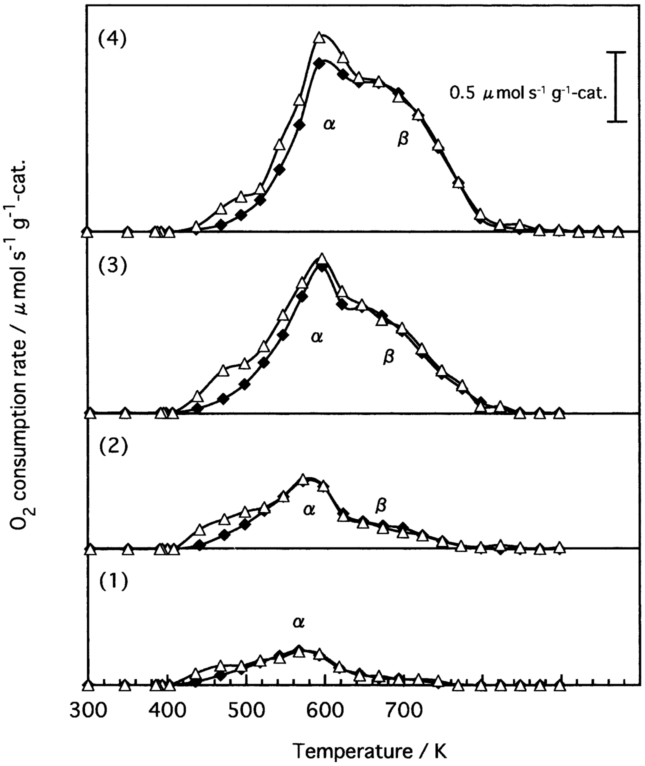

Fig. 4. TPO curves of the carbonaceous deposit accumulated on Fe-ZSM-5 (3.4 wt% Fe) during the N_2O reduction by C_2H_4 at 598 K for (1) 5 min, (2) 15 min, (3) 60 min, and (4) 120 min (△, the total amount of O_2 consumption; ◆, the amount of O_2 consumed for oxidation of the carbonaceous deposits).

the absence of O_2 for 5, 15, 60, and 120 min. This figure gives the amounts of O_2 consumed: one (closed symbol) is for the oxidation of C included in the carbonaceous deposits, which is determined by the amount of CO evolved/2 + the amount of CO_2 evolved, and the other (open symbol) is the total amount of O_2 consumed during TPO. In the α-peak region, the total amount of O_2 consumption is larger than the amount of O_2 consumed for the formation of CO and CO_2. In the β-peak region, on the other hand, the amount of O_2 used for the oxidation of carbonaceous materials is actually identical to the total amount of O_2 consumption. These results suggest that in the α-region O_2 is consumed by the oxidation of not only C included in the carbonaceous materials but also others, which should be H since the formation of H_2O was detected by gas analysis as noted earlier. Table 1 shows the amounts of C and H that are estimated to be included in the carbonaceous deposits and determined from TPO results. The former is the amount of CO evolved/2 and the amount of CO_2 evolved and the latter is the difference between the total amount of O_2 consumed and the former. It is found that the H/C ratio of the α-peak is between 0.905 and 1.08. These results shown in Fig. 4 and Table 1 suggest that the composition of the carbonaceous material oxidized at α-peak region is represented by approximately CH, while the carbonaceous species oxidized at the β-peak region does not need any additional oxygen to produce CO and CO_2.

Table 1
The amounts of carbon and hydrogen evolved as CO_x and H_2O, respectively, and H/C ratio of carbonaceous deposit oxidized at α-peak region, which is accumulated during N_2O reduction by C_2H_4 for different times on stream at 598 K

Reaction time (min)	Carbon[a]	Hydrogen[a]	H/C (–)
5	0.402	0.364	0.905
15	0.704	0.760	1.08
60	1.31	1.34	1.02
120	1.39	1.42	1.02

Catalyst: Fe-ZSM-5 (3.4 wt% Fe), 0.05 g.
[a] Values are in mmol g_{cat}^{-1}.

Table 2
Carbonaceous deposit accumulated under various conditions

Catalyst	Reactant (ppm)			N_2O conversion	$C\alpha$ [a]	$C\beta$ [a]
	N_2O	C_2H_4	O_2	(%)		
Na-ZSM-5	2000	2000	0	0	0	0
Fe-ZSM-5	0	2000	0	–	Trace	Trace
Fe-ZSM-5	2000	2000	0	36.0	1.39	1.85
Fe-ZSM-5	2000	2000	5000	87.4	0	0.18

Catalyst: Na-ZSM-5 or Fe-ZSM-5 (3.4 wt% Fe), 0.05 g. Conditions: 598 K, 120 min.
[a] Values are in mmol g_{cat}^{-1}.

The reaction behavior of C_2H_4 has been studied over Na-ZSM-5 and Fe-ZSM-5 to elucidate the formation of carbonaceous deposits. Table 2 summarizes the results for the conversion of N_2O to N_2 and the amounts of $C\alpha$ and $C\beta$ formed on Na-ZSM-5 and Fe-ZSM-5 (3.4 wt% Fe) in the reaction of C_2H_4 (2000 ppm) at 598 K for 120 min. Over Na-ZSM-5, no reaction occurs between N_2O (2000 ppm) and C_2H_4 (2000 ppm) under these conditions and thus no carbonaceous deposit forms on the surface. Only a trace amount of carbonaceous deposit forms on Fe-ZSM-5 in contact with C_2H_4 (2000 ppm) alone. The reduction of N_2O (2000 ppm) by C_2H_4 (2000 ppm) proceeds over Fe-ZSM-5 and the carbonaceous deposits ($C\alpha$, $C\beta$) form on the surface in the absence of O_2, while $C\alpha$ disappears in the presence of 5000 ppm of O_2. These results suggest that the carbonaceous deposit would form on the site of Fe on the catalyst surface and the presence of N_2O is effective for the accumulation of the carbonaceous deposit.

The influence of Fe loading and the reaction temperature on the amounts of carbonaceous deposits is measured by means of the TPO method in a similar manner as shown in Figs. 2 and 3 and the results are summarized in Tables 3 and 4. Table 3 summarizes the influence of Fe loading (1.0, 1.8, and 3.4 wt%) and the reaction temperature (573, 598, and 623 K) on the amount of the carbonaceous deposits accumulated on Fe-ZSM-5 during the reduction of N_2O (2000 ppm) by C_2H_4 (2000 ppm) in the absence of O_2. It is found that the amounts of $C\alpha$ and $C\beta$ increase with an increase in the amount of Fe loading. The amount of $C\alpha$ formed on Fe-ZSM-5 (3.4 wt% Fe) is almost the same despite differences in reaction temperature, while that of $C\beta$ formed on Fe-ZSM-5 (3.4 wt% Fe) increases with an in-

Table 3
The amount of carbonaceous deposit accumulated during N_2O (2000 ppm) reduction using C_2H_4 (2000 ppm) in the absence of O_2

Fe-ZSM-5 (wt%)	Reaction temperature (K)	N_2O conversion (%)	$C\alpha$ [a]	$C\beta$ [a]
1.0	598	18.6	0.59	0.50
1.8	598	27.0	1.06	1.07
3.4	573	18.9	1.25	1.14
3.4	598	38.7	1.39	1.85
3.4	623	70.5	1.12	2.62

Catalyst: Fe-ZSM-5, 0.05 g. Conditions: 598 K, 120 min.
[a] Values are in mmol g_{cat}^{-1}.

Table 4
The amount of carbonaceous deposit accumulated during the reduction of N_2O using C_2H_4 at various partial pressures in the absence of O_2

Reactant (ppm)		N_2O conversion	$C\alpha$ [a]	$C\beta$ [a]
N_2O	C_2H_4	(%)		
2000	6000	32.5	1.38	2.09
2000	4000	33.1	1.31	1.65
2000	2000	38.7	1.39	1.85
4000	4000	27.1	1.33	2.31
6000	6000	21.9	1.39	2.93
12,000	2000	14.5	1.26	2.85

Catalyst: Fe-ZSM-5 (3.4 wt%), 0.05 g. Conditions: 598 K, 120 min.
[a] Values are in mmol g_{cat}^{-1}.

crease in the reaction temperature. Table 4 summarizes the influence of the partial pressure of N_2O (2000, 4000, 6000, and 12,000 ppm) and C_2H_4 (2000, 4000, and 6000 ppm) on the amount of the carbonaceous deposits formed on Fe-ZSM-5 (3.4 wt% Fe) in the reduction of N_2O by C_2H_4 in the absence of O_2. It is found that the amount of $C\alpha$ formed on Fe-ZSM-5 changes little with the partial pressure of reactants, while that of $C\beta$ increases with an increase in the partial pressure of C_2H_4. On the basis of the results shown in Tables 3 and 4, it is found that the amount of $C\alpha$ formed on Fe-ZSM-5 does not depend on the reaction conditions so much, while that of $C\beta$ increases with increases of both the partial pressure of C_2H_4 and the reaction temperature.

3.3. Actions of carbonaceous deposits and O_2 in N_2O reduction

The reduction of N_2O by C_2H_4 and the formation of $C\alpha$ and $C\beta$ deposits were further examined to clarify the effects of O_2 and the carbonaceous deposits on this reduction. The influence of O_2 on the conversion of N_2O to N_2 and the formation of carbonaceous deposits are summarized in Fig. 5. In Fig. 5, the amount of the carbonaceous deposit formed in the reduction of N_2O (2000 ppm) with C_2H_4 (2000 ppm) at 598 K for 2 h in the absence and presence of O_2 and the conversion of N_2O to N_2 are plotted against the partial pressure of O_2. It is seen that the amount of the carbonaceous deposit decreases with an increase in the partial pressure of O_2 between 0 and 5000 ppm O_2 and then it disappears at O_2 partial pressure above 10,000 ppm. N_2O conversion obtained at O_2 partial pressure below 1000 ppm is about 36%, while it increases with an increase in O_2 partial pressure up to 5000 ppm and then a maximum value of 87.4% is obtained at 5000 ppm O_2. The conversion of N_2O decreases with an increase in O_2 partial pressure above 5000 ppm. If these gaseous reactants react with each other completely, the scheme of stoichiometric reaction would be followed by:

$$N_2O + C_2H_4 + \tfrac{5}{2}O_2 \rightarrow N_2 + 2CO_2 + 2H_2O. \qquad (1)$$

In this case, for example, 2000 ppm N_2O, 2000 ppm C_2H_4, and 5000 ppm O_2 give the stoichiometric composition. When the reduction of N_2O proceeds under reductive composition below 5000 ppm O_2, the carbonaceous deposit would be accumulated on the catalysts continuously. On the other hand, when the reaction proceeds under oxidative composition above 5000 ppm O_2, the carbonaceous deposit could be oxidized to CO_2 or CO by gaseous oxygen immediately, while a large excess of oxygen above 10,000 ppm in the feed gas would act as an inhibitor for the reduction of N_2O, since a considerable extent of C_2H_4 reductant may be reacted with excess oxygen.

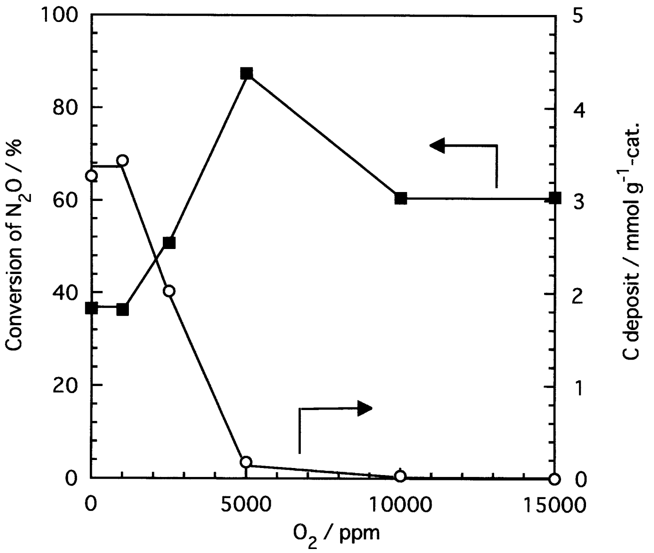

Fig. 5. The effects of O_2 partial pressure on the conversion of N_2O to N_2 and the amount of the carbonaceous deposit accumulated in the N_2O reduction by C_2H_4 at 598 K for 2 h (■, the conversion of N_2O to N_2; ○, the amount of the carbonaceous deposit).

The experiment for transient response of O_2 has been attempted to elucidate the action of O_2 on the reduction of N_2O with C_2H_4. Fig. 6 shows the results for the transient response of O_2 (5000 ppm) in the reduction of N_2O (2000 ppm) with C_2H_4 (2000 ppm) at 598 K. In Fig. 6A, the changes in the partial pressure of N_2 and the amount of the carbonaceous deposits ($C\alpha$, $C\beta$) accumulated during the reduction of N_2O by C_2H_4 are plotted against the reaction time. It is seen that the partial pressure of N_2 decreases with an increase in the amount of $C\alpha$. This strongly suggests that the formation of N_2 is obviously inhibited by the presence of $C\alpha$, while the activity of catalyst is not affected

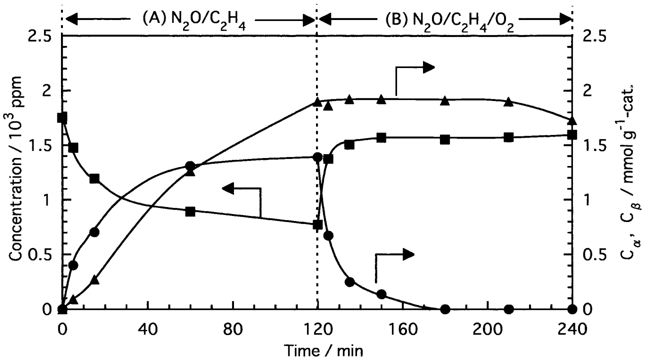

Fig. 6. The results for the transient response of O_2 (5000 ppm) in the reduction of N_2O (2000 ppm) by C_2H_4 (2000 ppm) at 598 K (■, the partial pressure of N_2 formation; ●, the amount of Cα; ▲, the amount of Cβ). (A, N_2O/C_2H_4; B, $N_2O/C_2H_4/O_2$.)

by the presence of Cβ. Fig. 6B shows the changes in the partial pressure of N_2 and the amount of Cα and Cβ obtained after the addition of O_2 (5000 ppm) into the reactants (N_2O, C_2H_4). When O_2 is added into the feed gas, the partial pressure of N_2 in the outflow increases rapidly and then gradually comes to a new steady-state value and the amount of Cα decreases rapidly and disappears within 60 min after the addition of O_2. On the other hand, the amount of Cβ remains constant as long as Cα exists on the catalyst, while Cβ decreases gradually after the disappearance of Cα. It is found from these results that the addition of O_2 into the reactants could take away the inhibitory effect of Cα on N_2O reduction, since Cα reacts rapidly with O_2 under the reaction conditions.

3.4. Characterization of carbonaceous deposits

The nature of Cα and Cβ deposits was further characterized by means of DRIFTS and XPS. The structure of carbonaceous deposits formed during the reduction of N_2O (8000 ppm) with C_2H_4 (8000 ppm) on Fe-ZSM-5 (3.4 wt% Fe) was studied by means of DRIFTS method. It is found that the absorption bands ascribed to C–H stretching of C=CH groups (3130, 3190 cm^{-1}) [26,27] are observed from 10 min after contact with the reaction gases and C=O groups (1740, 1780 cm^{-1}) [26,27] are observed after 30 min. These results suggest that carbonaceous species containing C–H groups formed on Fe-ZSM-5 at the initial stage of N_2O reduction and then another carbonaceous species containing C=O groups also formed on the catalyst. These findings correspond to the results for the composition of the carbonaceous materials estimated by TPO as shown in Fig. 4 and Table 1. Thus, the carbonaceous material oxidized at the α-peak region is represented by approximately CH, while that evolved at the β-peak region is expressed by C.

On the basis of XPS spectra measured on Fe-ZSM-5 (3.4 wt% Fe) used for the reduction of N_2O, it is found that the binding energies of the $Fe2p_{3/2}$ photoelectron are between 711.6 and 712.2 eV. The values are higher than those for bulk α-Fe_2O_3 (710.5 [30], 711.2 eV [31]) and Fe_3O_4 (710.5 [32], 711.2 eV [30]). This may indicate a strong interaction between iron and zeolite, and in fact, the binding energies of 711.6 and 712.1–712.3 eV are reported for iron incorporated in Fe-ZSM-5 [33] and Fe_2O_3–SiO_2 [29], respectively. These findings are supported by the data of X-ray powder diffraction and ^{57}Fe Mössbauer spectra. XRD patterns of Fe-ZSM-5 (3.4 wt% Fe) show no evidence for the presence of bulk α-Fe_2O_3 on the surface of catalyst and ^{57}Fe Mössbauer spectra of the catalyst show the presence of Fe^{3+} with tetrahedral coordination [34]. Fig. 7 shows XPS spectra of C 1s obtained over Fe-ZSM-5 catalysts used for the reduction of N_2O (2000 ppm) with C_2H_4 (2000 ppm) in the absence of O_2 at 598 K. Fig. 7 (1) shows C 1s spectrum obtained over Fe-ZSM-5 before reaction. Since the correction of the energy shift due to steady-state charging is accomplished by taking the C 1s line from adsorbed carbons at 284.5 eV [28,29] as an internal standard, this spectrum can be regarded as a background of the Fe-ZSM-5 catalyst used. The dotted curves shown in Fig. 7 (2) and (3) represent difference spectra between the solid curves shown in Fig. 7 (2) and (3) and that in Fig. 7 (1), respectively. Fig. 7 (2) shows C 1s spectrum obtained over Fe-ZSM-5 used for the N_2O reduction in the absence O_2 at 598 K for 15 min. It is found that the main peak (284.5 eV) increases slightly and the difference spectrum (283.6 eV) may indicate the formation of an isolated carbon [28]. Fig. 7 (3) shows C 1s spectra obtained over Fe-ZSM-5 used for the N_2O reduction in the absence of O_2 for 120 min. The main peak obtained by the N_2O reduction for 120 min is larger than that for 15 min. A shoulder peak represented by dashed line appears at 288.5 eV together with main peak and may be assigned as carboxylic groups [28]. Cβ species could be formed on the catalyst

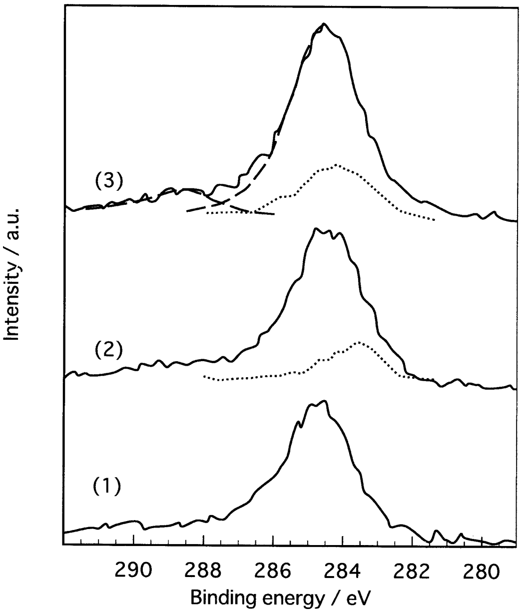

Fig. 7. XPS spectra of C 1s obtained over Fe-ZSM-5 catalysts used for the reduction of N_2O (2000 ppm) with C_2H_4 (2000 ppm) in the absence of O_2 at 598 K. Reaction conditions: (1) no reaction, (2) N_2O/C_2H_4, 15 min, (3) N_2O/C_2H_4, 120 min.

Table 5
Surface composition of Fe-ZSM-5 catalysts used for the reduction of N_2O (2000 ppm) by C_2H_4 (2000 ppm) in the absence of O_2 at 598 K as derived from XPS

Reactant composition	Reaction time (min)	Type of C deposit	Content (at%)						C/Fe (–)	C/Si (–)	Fe/Si (–)
			C	O	Al	Si	Fe	N			
(No reaction)		–	9.4	63.0	1.9	24.4	1.2	0.1	7.7	0.39	0.050
N_2O/C_2H_4	15	$C\alpha$	10.9	62.0	1.7	24.4	1.0	0.2	10.7	0.45	0.042
N_2O/C_2H_4	120	$C\alpha$, $C\beta$	15.6	58.7	1.7	23.0	0.75	0.3	20.8	0.68	0.033

surface by sufficient time reactions, and the carbonaceous species assigned as carboxylic groups can be regarded as $C\beta$ species derived by TPO.

The elemental compositions of the surface regions were investigated by means of XPS. The surface carbon, oxygen, aluminum, silicon, iron, and nitrogen contents are listed in Table 5, together with the reaction conditions of the N_2O reduction and the types of carbonaceous deposits derived by TPO. It is seen that the C content and surface C/Fe and C/Si ratios increase with an increase in the reaction time and, on the contrary, Fe and O contents and surface Fe/Si ratios decrease with an increase in the reaction time. These results suggest that the $C\alpha$ species, which is mainly formed at the initial stage of N_2O reduction, may be accumulated on the Fe site, since the Fe content decreases with the formation of $C\alpha$ while the Si content of ZSM-5 zeolite remains unaltered. On the other hand, $C\beta$ species may be accumulated on ZSM-5 zeolite surfaces, since the Si content on the surface as observed by XPS, as well as the Fe content, decreases by the N_2O reduction for 120 min.

4. Conclusions

The catalytic reduction of dinitrogen monoxide (N_2O) by ethylene (C_2H_4) in the absence and presence of O_2 is studied over Fe-ZSM-5 catalysts. The reduction of N_2O is fairly promoted by the presence of O_2. Two kinds of carbonaceous deposits ($C\alpha$, $C\beta$) classified by TPO are formed on Fe-ZSM-5 during the reduction of N_2O by C_2H_4 in the absence of O_2. $C\alpha$ species is formed at the initial stage of N_2O reduction and accumulated mainly on the Fe site, while $C\beta$ species is also accumulated on ZSM-5 zeolite surface. The catalytic activity of Fe-ZSM-5 decreases with an increase in the amount of $C\alpha$, while the catalytic activity is not affected by the presence of $C\beta$. The formation of these carbonaceous deposits is suppressed by the presence of O_2, and thus the catalytic reduction of N_2O by C_2H_4 is obviously promoted by the presence of O_2.

Acknowledgment

The authors thank to Prof. T. Kozaki (Hokkaido University) for performing the ^{57}Fe Mössbauer experiments.

References

[1] Y. Li, J.N. Armor, Appl. Catal. B 1 (1991) L21.
[2] T. Turek, Appl. Catal. B 9 (1996) 201; J. Catal. 174 (1998) 98.
[3] F. Kapteijin, M. Marban, J. Rodriguez-Mirasol, J.A. Moulijn, J. Catal. 167 (1997) 256.
[4] J.P. Ramírez, J. Overeijnder, F. Kapteijin, J.A. Moulijn, Appl. Catal. B 23 (1999) 59.
[5] M. Shimokawabe, K. Hirano, N. Takezawa, Catal. Today 45 (1998) 117.
[6] El-M. El-Malki, R.A. van Santen, W.H.M. Sachtler, Micropor. Mesopor. Mater. 35–36 (2000) 235.
[7] Y. Li, J.N. Armor, Appl. Catal. B 3 (1993) 55.
[8] M. Kögel, V.H. Sandoval, W. Schwieger, A. Tissler, T. Turek, Catal. Lett. 51 (1998) 23.
[9] C. Pophal, T. Yogo, K. Tanabe, K. Segawa, Catal. Lett. 44 (1997) 271.
[10] C. Pophal, T. Yogo, K. Yamada, K. Segawa, Appl. Catal. B 16 (1998) 177.
[11] K. Yamada, S. Kondo, K. Segawa, Micropor. Mesopor. Mater. 35–36 (2000) 227.
[12] M. Shimokawabe, N. Takahata, T. Chaki, N. Takezawa, React. Kinet. Catal. Lett. 71 (2000) 313.
[13] S. Kameoka, T. Suzuki, K. Yazaki, S. Tanaka, S. Ito, T. Miyadera, K. Kunimori, Chem. Commun. (2000) 745.
[14] S. Kameoka, K. Yazaki, T. Takeda, S. Tanaka, S. Ito, T. Miyadera, K. Kunimori, Phys. Chem. Chem. Phys. 3 (2001) 256.
[15] S. Kameoka, K. Kita, S. Tanaka, T. Nobukawa, S. Ito, K. Tomishige, T. Miyadera, K. Kunimori, Catal. Lett. 79 (2002) 63.
[16] Z.H. Zhu, G.Q. Lu, Dev. Chem. Eng. Min. Process. 7 (1998) 563.
[17] Z.H. Zhu, L. Finnerty, G.Q. Lu, R.T. Yang, J. Phys. Chem. B 105 (2001) 821.
[18] C.P. Byrne, R.T. Yang, Z.H. Zhu, G.Q. Lu, J. Phys. Chem. B 106 (2002) 2592.
[19] V.D. Belyaev, T.I. Politova, V.A. Sobyanin, Catal. Lett. 57 (1999) 43.
[20] J.H. Holles, M.A. Switzer, R.J. Davis, J. Catal. 190 (2000) 247.
[21] B. Coq, M. Mauvezin, G. Delahay, S. Kieger, J. Catal. 195 (2000) 298.
[22] B. Coq, M. Mauvezin, G. Delahay, J.-B. Butet, S. Kieger, Appl. Catal. B 27 (2000) 193.
[23] P. Gélin, M. Primet, Appl. Catal. B 39 (2002) 1.
[24] T.F. Garetto, C.R. Apesteguía, Catal. Today 62 (2000) 189.
[25] I.M. Kennedy, Prog. Energy Combust. Sci. 23 (1997) 95.
[26] L.H. Little, Infrared Spectra of Adsorbed Species, Academic Press, London, 1966.
[27] A.D. Cross, An Introduction to Practical Infra-red Spectroscopy, 2nd ed., Butterworth, London, 1964.
[28] N.M. Rodriguez, P.E. Anderson, A. Wootsch, U. Wild, R. Schlögl, Z. Paál, J. Catal. 197 (2001) 365.
[29] P. Fabrizioli, T. Bürgi, M. Burgener, S. van Doorslaer, A. Baiker, J. Mater. Chem. 12 (2002) 619.
[30] K. Hirokawa, M. Oku, Talanta 26 (1979) 855.
[31] C.R. Brundle, T.J. Chuang, K. Wandelt, Surf. Sci. 68 (1977) 459.
[32] T.J. Udovic, J.A. Dumesic, J. Catal. 89 (1984) 303.
[33] R.B. Borade, A. Adnot, S. Kaliaguine, Zeolites 11 (1991) 710.
[34] K. Lázár, G. Borbély, H. Beyer, Zeolites 11 (1991) 214.